Fano resonance in discrete lattice models: controlling lineshapes with impurities

Arunava Chakrabarti†
Max-Planck-Institut für Physik komplexer Systeme
Nöthnitzer Strasse 38, Dresden 01187, Germany

Abstract

The possibility of controlling Fano lineshapes in the electronic transmission is addressed in terms of a simple discrete model within a tight binding framework, in which a finite sized ordered chain is coupled from one side to an infinite linear chain (the 'backbone') at one lattice point. It is found that, the profile of Fano resonance is strongly influenced by the presence of impurity atoms in the backbone. We specifically discuss the case with just two substitutional impurities sitting in the otherwise ordered backbone. Precise analytical formulae relating the locations of these impurities to the size of the side coupled chain have been presented. The nature of the transmission spectrum and the reversal of the pole-zero structures in the Fano resonance are discussed with the help of these formulae.

PACS numbers: 42.25.Bs, 42.65.Pc, 61.44.-n, 71.23.An, 72.15.Rn, 73.20.Jc
Keywords: Fano resonance, Tight binding models

1. Introduction

The Fano resonance usually refers to a sharp asymmetric profile in the transmission or absorption spectrum and, is common to many physical systems including the absorption of light by atomic systems [1], Aharonov-Bohm interferometers [2]-[3], quantum dots [4]-[6], propagation of light through photonic crystal waveguides [7]-[9]. A Fano profile in the transmission (absorption) spectrum is caused by the formation of a discrete energy level in a continuum, and there is interaction between the two. A defect present in the system is capable of creating such a discrete level. It also provides additional paths in the wave scattering [10]. The resulting constructive or destructive interference gives rise to either perfect transmission or complete reflection producing a sharp asymmetric lineshape. Fano [1] derived this lineshape as,

$$\mathcal{F}(\epsilon) = \frac{(\epsilon + \eta)^2}{\epsilon^2 + 1} \tag{1}$$

where, $\epsilon = (E - E_R)/(\Gamma/2)$ with E_R being the 'resonance energy' and Γ the line width. η is the asymmetry parameter.

In recent times, it has been demonstrated that, simple discrete lattice models with side coupled impurities also exhibit Fano profiles in the transmission spectrum [11]-[12]. Discrete models are important, particularly in the context of commendable advancement of miniaturization techniques, as in many cases they serve the purpose of understanding some salient features of electronic transport in mesoscopic systems. For example, the electronic transmission through a non-interacting tight binding chain with an interacting *side coupled* quantum dot was examined by Torio et al [13] to investigate the Kondo resonance and Fano anti-resonances in the transport through quantum dots. Rodríguez et al [14] modelled a quantum wire attached to a quantum dot at one lattice point by a simple discrete tight binding hamiltonian and studied the dynamics of electron transport. Fano resonances and Dicke effect [15] in quantum wire with side coupled quantum dots have been studied, again within a tight binding formalism and independent electron approximation, by Guevara et al [16] and Orellana et al [17]. Interestingly, Papadopoulos et al [18] have addressed the possibility of controlling electron transport through Fano resonances in molecular wires using a first principles approach. Once again, the generic features of the transport properties have been captured with the help of a discrete lattice model.

The simplest model which describes the essential features of the coupling between a discrete state and a continuum is the Fano-Anderson model [19]. In such a model, one takes a one dimensional ordered lattice and fixes, from one side, a 'hanging' impurity, which may consist of a single atomic site [11] or a chain with multiple sites [12]. The system is described by a tight binding hamiltonian, and the role of the 'coupling' between the continuum and the discrete levels is played by the hopping integral connecting the ordered backbone and the first site of the defect system. Such a linear chain with a side coupled defect was addressed earlier [20], but the focus was to understand the effect of such a 'geometrical defect' on the electronic spectrum and localization properties. Recently, the transmission profile has been examined [21] when the defect chain is a quasiperiodic Fibonacci lattice, which offers a multifractal Cantor set spectrum as the chain length becomes infinity. The trans-

mission windows have been found to be punctuated by zeros of transmission, the distribution resembling a self similar fractal as the attached quasiperiodic defect chain becomes larger and larger.

A very interesting feature in the transmission spectrum of a linear ordered chain with a side coupled atom or a chain of atoms [12] is a swapping of the peak-dip (pole-zero) profile of the Fano resonance at special values of the energy of the electron. In a discrete model, the swapping is found to be associated with the presence of an additional defect (apart from the side coupled one) in the ordered backbone. This additional defect may be a single substitutional *impurity* sitting 'on' the backbone [12], or another chain of atoms connected to a different lattice point [21]. The important thing here is that, the swapping of the peak-dip profile can be controlled by adjusting the number of atoms in the ordered backbone which separate the hanging Fano defect chain from the impurity [21]. That is, the control parameter here is a discrete variable in contrast to previous studies [22]-[23] where one had to vary continuous parameters such as the strength of the impurity potential or the magnetic field to see such an effect. The significance of such swapping has already been appreciated in the literature [24]. For example, if similar reversal of peak position happens even with a magnetic impurity, then the transmission peak of the spin 'up' (down) electron may coincide with the transmission zero of the spin 'down' (up) electron, making the system behave as a *spin filter*. Incidentally, a tight binding model of a quantum wire with an attached ring has been proposed as a model of a spin filter [25] and another discrete T-stub structure has very recently been examined as a potential candidate for a spin-splitting device [26].

In this context, the possibility of controlling the Fano profiles by placing impurities on the backbone becomes an interesting issue. This important aspect has received very little attention, specially in the context of a discrete lattice model. This precisely is the idea which motivates us to look deeper into the problem of tuning Fano lineshapes in a discrete lattice model. In this communication, we present the first step taken by us to look into the effect of placing more than one impurity in the ordered backbone on the transmission lineshapes. Secondly, we examine carefully whether there is a correlation between the 'size' of the side coupled Fano-Anderson (FA) defect and the separation between the impurities on the ordered backbone. These aspects may turn out to be important in gaining control over the Fano profiles in the transmission, particularly, over a possible reversal of the peak-dip profile.

We get extremely interesting results. In this paper we present analytical results with just two impurities sitting symmetrically on the backbone N sites away from the lattice point at which the defect chain of n sites is side attached (Fig.1). We show, that there is a definite correlation between the numbers N and n which controls the transmission spectrum in a *completely predictable* way. This is also intimately connected to the signs of the impurity potentials. We provide a prescription to predict the principal features of the transmission spectrum and the possibility of securing a full control over the reversal of the peak-dip structures. This aspect, to the best of our knowledge, has not been addressed before. In what follows, we describe the model and the method in section 2. Sections 3 and 4 contain the results and the discussion and, in section 5 we draw conclusions.

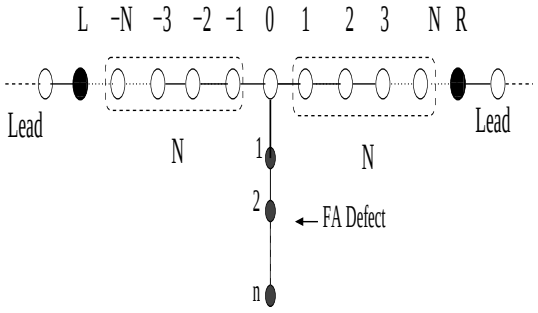

FIG. 1: A Fano-Anderson (FA) defect coupled to a discrete chain (the backbone) at one site (marked 'zero'). The two 'impurities' ('L' and 'R') are marked by solid circles on the backbone.

2. The Model and the method

Let us refer to Fig.1. The backbone (model quantum wire) consists of periodically placed identical sites (open circles) excepting two 'impurities' (solid black circle), each being separated from the zeroth site by N sites of the ordered chain. At the zeroth site of the backbone a n-site Fano-Anderson (FA) chain is attached, which we shall refer to as the FA defect. Beyond the impurities (black circles on the backbone), the remaining portions of the backbone serve as the 'leads' along which an electron enters the system, and leaves it as well. The FA defect plays the role of a resonant cavity sustaining standing waves [11]. In one of the first papers on similar problems, the influence of a grafted stub in a quantum wire in obtaining Fano resonance was discussed earlier, using the continuous version of the Schrödinger equation by Tekman and Bagwell [27].

The Hamiltonian of the system, in the standard tight binding form, is written as,

$$H = H_W + H_D + H_{WD} \tag{2}$$

where,

$$\begin{aligned} H_W &= \sum_{i=-\infty}^{\infty} \epsilon_i c_i^\dagger c_i + t_0 \sum_{<ij>} c_i^\dagger c_j \\ H_D &= \sum_{i=1}^{n} \epsilon_i d_i^\dagger d_i + \sum_{<ij>} t_{ij} d_i^\dagger d_j \\ H_{WD} &= \lambda(c_0^\dagger d_1 + d_1^\dagger c_0) \end{aligned} \quad (3)$$

In the above, $c^\dagger(c)$ and $d^\dagger(d)$ represent the creation (annihilation) operators for the wire and the defect respectively. The on-site potentials on the ordered backbone are, $\epsilon_i = \mu_L$ for the left (L) impurity, and $\epsilon_i = \mu_R$ for the right (R) impurity, and $\epsilon_i = \epsilon_0$ for the rest of the chain, as well as for every site of the FA defect. t_0 is the constant hopping integral in the periodic array of sites, which is our 'wire'. For all the results in this paper we assign the same hopping integral t_0 among the sites in the bulk of the FA defect. The first site of the FA defect is coupled to the zeroth site of the backbone via a hopping integral λ. So, λ is the 'interaction' which locally couples the two subsystems, viz, the periodic chain, and the dangling defect. If we decouple the two, the spectrum of the periodic quantum wire is absolutely continuous, the band extending from $\epsilon_0 - 2t_0$ to $\epsilon_0 + 2t_0$. The dispersion relation is $E = \epsilon_0 + 2t_0 \cos qa$, a representing the lattice spacing. With non-zero λ it is not right to view the two subsystems separately. In this case, the defect chain may be looked upon as a single impurity with a complicated internal structure and located at a single site marked 'zero' in the backbone (Fig.1). Therefore, while examining the transmission across the impurity, one has to be careful to adjudge whether the concerned energy really belongs to the spectrum of the entire system, that is, the ordered backbone plus the FA defect.

To calculate the electronic transmission across such a system, we first of all 'wrap' the hanging FA defect to create an effective defect site with an energy dependent on site potential ϵ^* at the lattice point marked zero. This is easily done by making use of the set of difference equations

$$\begin{aligned} (E-\epsilon_0)\psi_1 &= \lambda\psi_{0(Backbone)} + t_0\psi_2 \\ (E-\epsilon_0)\psi_j &= t_0(\psi_{j-1} + \psi_{j+1}) \\ (E-\epsilon_n)\psi_n &= t_0\psi_{n-1} \end{aligned} \quad (4)$$

for all sites of the FA defect chain with $2 \leq j \leq n-1$ corresponding to the middle equation, and then eliminating all the individual amplitudes ψ_j with $j = 1$ to n sequentially in terms of the site number zero in the backbone. Using this decimation renormalization method [21], [28], the effective (renormalized) on site potential ϵ^* at the zeroth site of the backbone is given by,

$$\epsilon^* = \epsilon_0 + \frac{\lambda^2}{E - \tilde{\epsilon}} \quad (5)$$

where,

$$\tilde{\epsilon} = \epsilon_0 + \frac{t_0 U_{n-3}(x)}{U_{n-2}(x)} + \frac{t_0^2}{U_{n-2}^2(x)} \frac{1}{E - \epsilon_0 - \frac{t_0 U_{n-3}(x)}{U_{n-2}(x)}} \quad (6)$$

for $n \geq 2$. Here, $x = (E - \epsilon_0)/2t_0$ and $U_n(x)$ is the nth order Chebyshev polynomial of the second kind. The problem is now reduced to the calculation of transmission across a linear array of three impurities with on-site potentials μ_L, ϵ^* and μ_R occupying lattice coordinates $-N$, 0 and N respectively. The result is,

$$T = |\tau^2| \quad (7)$$

with the transmission 'amplitude' τ given by [29],

$$\tau = e^{-i\theta(q,N)} \frac{2\sin qa}{\alpha + i\beta} \quad (8)$$

Here,

$$\begin{aligned} \alpha &= (M_{11} - M_{12})\sin qa - M_{22}\sin 2qa \\ \beta &= M_{11} + (M_{12} - M_{21})\cos qa - M_{22}\cos 2qa \end{aligned} \quad (9)$$

and, q and a are the wave vector and the lattice spacing respectively. We shall take $a = 1$ in all the calculations which follow. $\theta(q, N)$ is a phase factor, whose explicit form is not displayed as it will not be needed for our purpose. M_{ij} are the elements of the transfer matrix,

$$M = M_R . M_{Cent} . M_L \quad (10)$$

where,

$$M_{R(L)} = \begin{pmatrix} \frac{E-\mu_{R(L)}}{t_0} & -1 \\ 1 & 0 \end{pmatrix}. \quad (11)$$

and,

$$M_{Cent} = \begin{pmatrix} U_N(x) & -U_{N-1}(x) \\ U_{N-1}(x) & -U_{N-2}(x) \end{pmatrix} . \begin{pmatrix} (E-\epsilon^*)/t_0 & -1 \\ 1 & 0 \end{pmatrix} . \begin{pmatrix} U_N(x) & -U_{N-1}(x) \\ U_{N-1}(x) & -U_{N-2}(x) \end{pmatrix}. \quad (12)$$

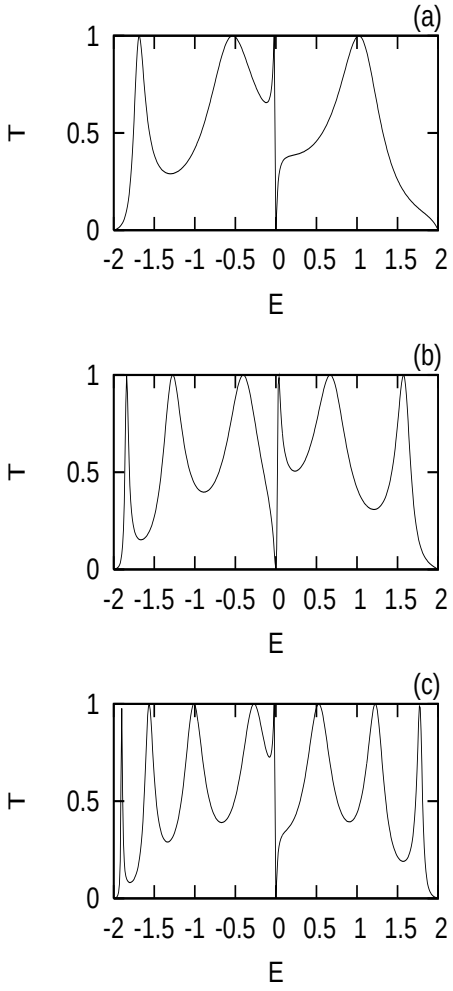

FIG. 2: The transmission coefficient for single atom FA defect. The two impurities on the backbone have identical signs, viz, $\mu = +1$ for each of them. We have taken $\epsilon_0 = 0$, $t_0 = 1$ and $\lambda = 0.2$ in unit of t_0. The peak-dip profile at $E = \epsilon_0 = 0$ in (a) ($N = 1$) is swapped into a dip-peak structure in (b) ($N = 2$), and is reversed in (c) ($N = 3$).

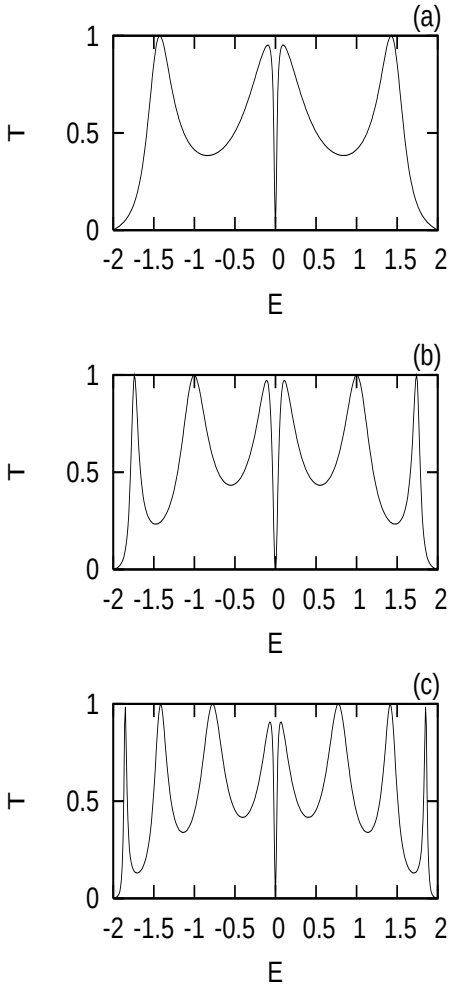

FIG. 3: The transmission coefficient (T) against energy for single atom FA defect when the impurity-potentials on the backbone are set equal to $\mu = +1$ and $\mu = -1$ for the left (L) and the right (R) impurities respectively. Other parameters are the same as in Fig.2.

3. Results and discussion

The general features of the transmission spectra for various values of N and n are presented in Fig.2 to Fig.5. To justify the spirit of this work, we discuss specifically Fano lineshape in the transmission and their reversal at special energies. The influence of the signs of the impurity potentials $\mu_{L(R)}$ are also addressed. To simplify matters, we set $|\mu_L| = |\mu_R| = \mu$, and to have a clear understanding of the arguments we present analytical results when the FA defect is just a single atom. The extension to the cases of multi-atom FA defect is trivial, only difference is that then we have more than one energy at which the reversal of the peak-dip profile takes place.

3.1 The repulsive impurity: $\mu > 0$

With just one atom as FA defect ($n = 1$), at $E = \epsilon_0$, we get $\epsilon^* = \infty$ resulting in $T = 0$, an anti-resonance. The spectrum for $N = 1$, 2 and 3, has been shown in Fig.2. The peak-dip (pole-zero) structure in the spectrum and

its reversal with N is clear at the anti-resonance energy. To get an analytical insight into the effect of changing N, we expand τ in Eq.(8) around $E = \epsilon_0$ by setting $E = \epsilon_0 + \delta$, and drop terms smaller than those of the order of δ. The result, apart from the trivial phase factor in Eq.(8), is,

$$\tau \simeq \frac{(2t_0^3 \sin qa)\delta}{t_0 \mathcal{F}(N)\left[\delta + \frac{\mathcal{G}(N)}{\mathcal{F}(N)}\right] + i\mathcal{H}(N)\left[\delta + \frac{\mathcal{K}(N)}{\mathcal{H}(N)}\right]} \qquad (13)$$

where, $\mathcal{F}(N) = \lambda^2 U_N^2 - 2t_0^2(U_{N-1}^2 + U_N U_{N-2}) + 4t_0\Delta U_N U_{N-1}$, $\mathcal{G}(N) = 2\lambda^2 U_N(\Delta U_N - t_0 U_{N-1})$, $\mathcal{H}(N) = \lambda^2 t_0 U_N U_{N-1} + 2t_0^3 U_{N-1}(U_N - U_{N-2}) - \Delta\lambda^2 U_N^2 + 2t_0^2\Delta(U_{N-1}^2 + U_N U_{N-2}) - 2t_0\Delta^2 U_N U_{N-1}$, and $\mathcal{K}(N) = \lambda^2[t_0^2(U_N^2 - U_{N-1}^2) - \Delta^2 U_N^2 + 2t_0\Delta U_N U_{N-1}]$. We have set $\Delta = \epsilon_0 - \mu$. All the quantities $\mathcal{F}$, $\mathcal{G}$, $\mathcal{H}$, and $\mathcal{K}$, and the wave vector q have to be evaluated at the δ-neighbourhood of $E = \epsilon_0$, and Fig.2 corresponds to the case where $\epsilon_0 = 0$ and $\mu = +1$.

The expression of the transmission amplitude reveals that the zero of transmission is at $\delta = 0$, while the real part in the denominator becomes zero when $\delta = -\mathcal{G}(N)/\mathcal{F}(N)$. Thus the locations of the two zeros are different. Similar observations were made earlier in the case of a mesoscopic two-lead ring [24]. These detuned but concomitant zeros result in a non zero asymmetry parameter and an asymmetric Fano lineshape [30] at $E = \epsilon_0$. The interesting fact about the ratio $\mathcal{G}(N)/\mathcal{F}(N)$ is that, it flips sign as N changes. This results in a swapping of the peak-dip profile. For example, when $\mathcal{G}(N)/\mathcal{F}(N) < 0$, then the peak of the transmission follows the dip. On the other hand, for $\mathcal{G}(N)/\mathcal{F}(N) > 0$, the peak precedes the dip. This precisely happens in Fig.2, where the peak→dip structure for $N = 1$ is reversed into a dip→peak one for $N = 2$ at $E = \epsilon_0$. The profile of Fano resonance is of course restored as N is increased to the value 3. The sign-flip continues with N increasing sequentially (an odd-even effect in terms of N), as can be checked by calculating $\mathcal{G}(N)/\mathcal{F}(N)$ for successive values of N, with $n = 1$. It is also apparent that, apart from the sharp Fano resonance at $E = \epsilon_0$, there will be other transmission peaks arising out of the typical Fabry-Perot type interference effects as the incoming wave interferes constructively in between the impurity sites.

With $\mu = -1$, the entire spectrum is a mirror image (with respect to the centre of the spectrum) of Fig.2. So, we move on to the next non-trivial case.

3.2 One attractive and one repulsive impurity: $\mu_L = -\mu$ and $\mu_R = +\mu$

We now discuss the case when the on-site potentials of the left and the right impurities are equal in magnitude, but opposite in sign. That is, Δ has the same magnitude for the left and right impurities. Only the sign of Δ is opposite for them. In this case, an expansion of the transmission amplitude around $E = \epsilon_0$ as done earlier leads to the result (again dropping the unimportant phase factor),

$$\tau \simeq \frac{(2t_0^3 \sin qa)\delta}{t_0 \Theta(N)\left[\delta - \frac{\Phi(N)}{\Theta(N)}\right] + i\left[\delta\Gamma_1 + \Gamma_2\right]} \qquad (14)$$

where, $\Theta(N) = \lambda^2 U_N^2 - 2t_0^2(U_{N-1}^2 + U_N U_{N-2})$, $\Phi = 2t_0\lambda^2 U_N U_{N-1}$, $\Gamma_1 = 2t_0\Delta^2 U_N U_{N-1} + 2t_0^3 U_{N-1}(U_N - U_{N-2}) + \lambda^2 t_0 U_N U_{N-1}$ and, $\Gamma_2 = \lambda^2[\Delta^2 U_N^2 + t_0^2(U_N^2 - U_{N-1}^2)]$. It is obvious that the zero of transmission occurs again at $\delta = 0$, while the possibility of a peak-dip reversal is there if the ratio $\Phi(N)/\Theta(N)$ flips sign as N changes. Here, in this case, it can be verified that the ratio $\Phi(N)/\Theta(N)$ *does not* change sign as N increases. This implies, a swapping of the peak-dip profile of the Fano resonance at $E = \epsilon_0$ is *not possible* in this case. The peak always remains on one side of the dip for a fixed sign of δ. In addition to this, it is to be appreciated that the ratio $\Phi(N)/\Theta(N)$ is independent of Δ, and yields identical values for $E - \epsilon_0 = \pm\delta$. This explains the completely symmetrical pattern in the transmission coefficient immediately around $E = \epsilon_0$ in Fig.3. In fact, the entire spectrum in this case is symmetric around the centre, i.e. around $E = \epsilon_0$, a fact that of course, is due to the same choice of the value of the on-site potential for the FA defect and the backbone (except the impurities).

4. More atoms in the FA defect: correlation between 'N' and 'n'

We now turn to the cases when one has got more atoms in the FA defect. The basic question we ask is that, whether the swapping of the zero-pole structure in the Fano profile remains a generic feature of the transmission, independent of N and n . Now we shall have n eigenvalues for an n-site FA defect at which the transmission coefficient vanishes. One has to do the exercise outlined in the previous section for each of these eigenvalues, which is not difficult, but tiring. Instead, we present results of systematic evaluation of T for several such cases, from which we have been able to work out the precise criterion for the existence of a reversal of the sharp asymmetry in the peak-dip profile. The formulae have been numerically checked by changing N and n at our will and have been verified analytically for small values of N and n. The formulae are found consistent with the transmission spectra for all (N, n) combinations we examined.

We begin with $n = 2$ and only discuss the case when the left and the right impurities have the same magnitude, but opposite sign. That is, we have a repulsive and

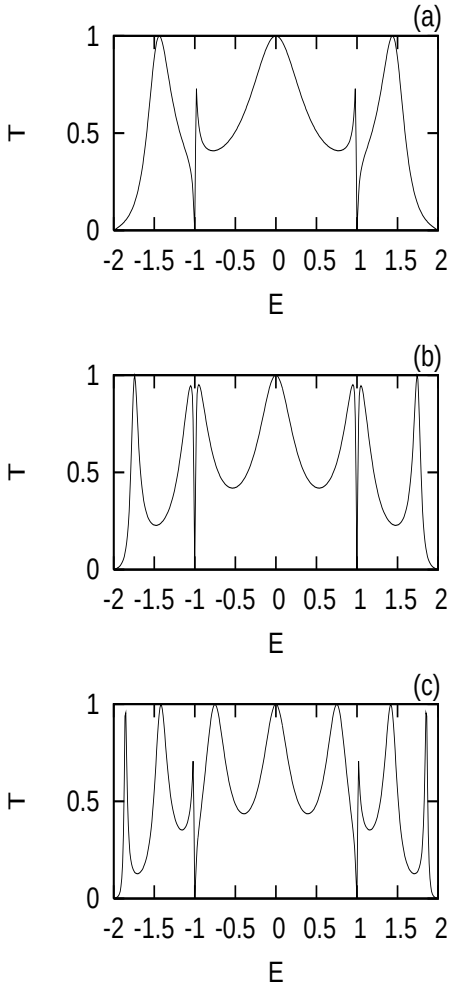

FIG. 4: The swapping of peak-dip profile and the N-dependence of transmission when the side coupled defect chain contains two atoms ($n = 2$). Here, $\mu_L = 1$ and $\mu_R = -1$ for the left and the right impurity respectively. $N = 1$, 2 and 3 in figures (a), (b) and (c) respectively. The values of on-site potentials and the hopping integrals are as in Fig.3, and $\lambda = 0.2$ in unit of t_0.

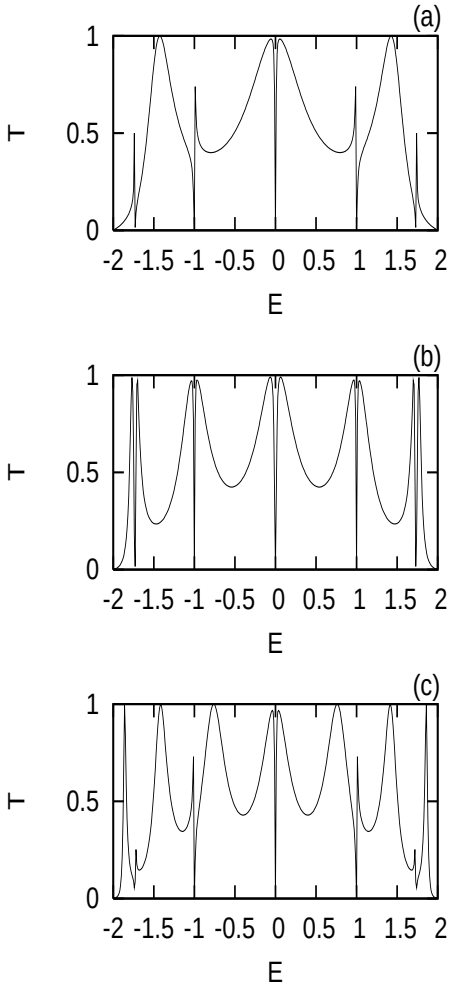

FIG. 5: The swapping of peak-dip profile and the N-dependence of transmission when the side coupled defect chain contains five atoms ($n = 5$). $N = 1$, 2, 3 in figures (a), (b) and (c) respectively, and the other parameters are same as in Fig.4.

an attractive potential sitting as impurities on the backbone. We also set the FA defect-wire coupling at a relatively small value to make the asymmetric jumps in the spectrum sharp. The two atoms in the FA defect have the same on site potential ϵ_0 and the hopping integral is t_0 everywhere. While in all cases the spectrum is mirror symmetric around $E = \epsilon_0$ with a transmission zero showing up at the centre of the spectrum, we observe remarkable changes at other parts of the spectrum as N is changed sequentially. This is illustrated in Fig.4 for a weak FA defect-wire coupling λ. For $N = 1$, two sharp asymmetric Fano resonances are observed at $E = \epsilon_0 \pm t_0$ which are the eigenvalues of an isolated two-atom chain. A dip-peak structure appears at $E = \epsilon_0 - t_0$, while a peak-dip profile is seen at $E = \epsilon_0 + t_0$. With $N = 2$, the asymmetric Fano lineshapes at $E = \epsilon_0 \pm t_0$ *totally disappear* and are replaced by *almost* symmetric anti-resonances. We use the word 'almost' because with smaller values of λ, the transmission anti-resonances become more and more symmetric looking, while with increasing λ, the width of the anti-resonance increases, and the Fano anti-resonance deviates from a symmetric appearance as we move away from the special energies. The overall mirror symmetry of the spectrum persists. By changing N from 2 to 3 we restore the asymmetric structure in the transmission

spectrum around $E = \epsilon_0 \pm t_0$, but now, remarkably, the sharp peak-dip profiles are found swapped with respect to the $N = 1$ case. In this way, with $n = 2$, we have checked that there is *no swapping of the transmission profile* (this is important to appreciate) if we set $N = 2$, 5, 8 etc, though the *symmetric* look of the transmission anti-resonances are controlled by the strength of the coupling λ. Reversal of the peak-dip profile occurs for other values of N. In Fig.5 we present results for $n = 5$. At $E = \epsilon_0 \pm t_0$ and $E = \epsilon_0 \pm \sqrt{3}t_0$, we find sharp asymmetric Fano lineshapes for $N = 1$ which disappear as N changes to 2. With $N = 3$ the sharp (local) asymmetry in lineshapes around the above energies is back, but now the peak-dip sequence is swapped. Multiple resonances appear in between. The jump at the extreme values like $E = \epsilon \pm \sqrt{3}t_0$ appears smaller, but the (local) asymmetry and the sharpness are apparent. We have carried out extensive numerical evaluation of the transmission spectrum by changing n and N and for the case when the left and the right impurity potentials have same magnitude, but different signs. The results can be summarized in two different formulae which have been verified with arbitrary combination of N and n. The results are the following.

(a) For even number of atoms n in the FA defect, the transmission spectrum will exhibit *no asymmetric peak-dip (or, dip-peak) profile* when we select N in such a way that,

$$N_l = (n + 1)l - 1 \tag{15}$$

with $n = 2$, 4, 6, etc., and $l = 1$, 2, 3, ...

(b) When n is odd, the formula is,

$$N_l = \left(\frac{n+1}{2}\right) l - 1 \tag{16}$$

for $n \geq 3$ and l again being equal to 1, 2, 3, etc.

Before ending this section, we would like to mention that we have also investigated other combinations of (N, n) and the their interplay with the signs and the magnitudes of the impurity potential μ. Results indicate the presence of both symmetric and asymmetric Fano lineshapes in the transmission spectrum in general. The reversal of peak-dip structure takes place as N changes sequentially. For example, with $\mu_L = \mu_R = \mu > 0$, and $n = 2$, the spectrum consists of a sharp asymmetric Fano anti-resonance with a dip-peak (zero-pole) jump at $E = \epsilon_0 - t_0$ and a symmetric transmission zero at $E = \epsilon + t_0$ if we start with $N = 1$. With $N = 2$, the spectrum exhibits only asymmetric profiles at the two above energies, with the earlier dip-peak shape at $E = \epsilon - t_0$ being swapped into a peak-dip structure. The symmetric lineshape at $E = \epsilon_0 + t_0$ is now replaced by an asymmetric peak-dip drop. The spectrum is not symmetric on the whole around the centre, i.e. around $E = \epsilon_0$. Such variations have been studied with supporting analytical formulae for various combinations of N, n and μ. However, we do not show every such case separately to save space.

5. Conclusions

In conclusion, we have examined the occurrence of Fano lineshapes in a discrete model within a tight binding framework using analytical and numerical methods. We have shown that by placing more than one substitutional impurity in the backbone lattice we can control the Fano lineshapes in a completely predictable way. We provide exact formulae which guide us to choose appropriate combination of the placement of the impurities and the size of the side coupled Fano defect for which we either retain, or get rid of the swapping of the asymmetric Fano profiles in the transmission spectrum. Two specific cases have been presented to explain our idea. This simple model may help in choosing an appropriate combination of the defect's size and the impurity-locations in a quantum wire to gain control over resonance lineshapes. It would be interesting to see if similar lineshapes are observed if one incorporates spin in such discrete models, in which case observing a 'spin filtering' effect in such discrete models may not be a remote possibility. Work in this direction is currently in progress.

Acknowledgments

I am grateful to the Max-Planck-Institute für Physik komplexer Systeme in Dresden for their hospitality and financial support during the course of this work. I acknowledge discussions with Sergej Flach and thank him for bringing several important references to my notice. I am also thankful to Ricardo Pinto for a careful reading of the manuscript and many constructive criticisms.

References

† On leave from Department of Physics, University of Kalyani, Kalyani, West Bengal 741 235, India. E-Mail: arunava@klyuniv.ernet.in

[1] U. Fano, Phys. Rev. 124 (1961) 1866.

[2] J. U. Nöckel, A. D. Stone, Phys. Rev. B 50 (1994)

17415.

[3] K. Kobayashi, H. Aikawa, S. Katsumoto, Y. Iye, Phys. Rev. Lett. 88 (2002) 256806.

[4] J. Göres, D. Goldhaber-Gordon, S. Heemeyer, M. A. Kastner, H. Shtrikman, D. Mahalu, U. Meriav, Phys. Rev. B 62 (2000) 2188.

[5] B. R. Bulka, P. Stefanski, Phys. Rev. Lett. 86 (2001) 5128.

[6] M. E. Torio, K. Hallberg, S. Flach, A. E. Miroshnichenko, M. Titov, Eur. Phys. J. B 37 (2004) 399.

[7] S. Fan, J. D. Joannopoulos, Phys. Rev. B 65 (2002) 235112.

[8] M. F. Yanik, S. H. Fan, M. Soljacic, Appl. Phys. Lett. 83 (2003) 2739.

[9] S. H. Fan, W. Suh, J. D. Joannopoulos, J. Opt. Soc. Am. B 20 (2003) 569.

[10] A. E. Miroshnichenko, S. F. Mingaleev, S. Flach, Y. S. Kivshar, Phys. Rev. E 71 (2005) 036626.

[11] P. Singha Deo, C. Basu, Phys. Rev. B 52 (1995) 10685.

[12] A. E. Miroshnichenko, Y. S. Kivshar, Phys. Rev. E 72 (2005) 056611.

[13] M. E. Torio, K. Hallberg, A. H. Ceccatto, C. R. Proetto, Phys. Rev. B 65 (2002) 085302.

[14] A. Rodríguez, F. Domínguez-adame, I. Gómez, P. A. Orellana, Phys. Lett. A 320 (2003) 242.

[15] R. H. Dicke, Phys. Rev. 89 (1953) 472.

[16] M. L. Ladrón de Guevara, F. Claro, P. A. Orellana, Phys. Rev. B 67 (2003) 195335.

[17] P. A. Orellana, F. Domínguez-Adame, E. diez, arXiv:cond-mat/0607094.

[18] T. A. Papadopoulos, I. M. Grace, C. J. Lambert, arXiv:cond-mat/0609109.

[19] G. D. Mahan, Many Particle Physics (1993) (New York, Plenum Press).

[20] F. Guinea, J. A. Vergeés, Phys. Rev. B 35 (1987) 979.

[21] A. Chakrabarti, To be published in Physical Review B.

[22] C. S. Kim, A. M. Satanin, Y. S. Joe, R. M. Cosby, Phys. Rev. B 60 (1999) 10962.

[23] M. L. Ladrón de Guevara, P. A. Orellana, Phys. Rev. B 73 (2006) 205303.

[24] Khee-Kyum Voo, C. S. Chu, Phys. Rev. B 72 (2005) 165307.

[25] M. Lee, C. Bruder, Phys. Rev. B 73 (2006) 085315.

[26] R. Wang, J. -Q. Liang, Phys. Rev. B 74 (2006) 144302.

[27] E. Tekman, P. F. Bagwell, Phys. Rev. B 48 (1993) 2553.

[28] B. W. Southern, A. A, Kumar, J. A. Ashraff, Phys. Rev. B 28 (1983) 1785.

[29] A. Douglas Stone, J. D. Joannopoulos, D. J. Chadi, Phys. Rev. B 24 (1981) 5583.

[30] S. Bandopadhyay, B. Dutta-Roy, H. S. Mani, Am. J. Phys. 72 (2004) 1501.